Effects of soldering temperature and preheating temperature on the properties of Sn–Zn solder alloys using wave soldering

Songtao Qu
Department of Global Supply Chain, Lenovo Group Ltd, Hefei, China
Qingyu Shi and Gong Zhang
School of Mechanical Engineering, Tsinghua University, Beijing, China, and
Xinhua Dong and Xiaohua Xu
Lenovo Group Ltd, Hefei, China

Abstract

Purpose – This study aims to address the problem of low-temperature wave soldering in industry production with Sn-9Zn-2.5 Bi-1.5In alloys and develop qualified process parameters. Sn–Zn eutectic alloys are lead-free solders applied in consumer electronics due to their low melting point, high strength, and low cost. In the electronic assembly industry, Sn–Zn eutectic alloys have great potential for use.

Design/methodology/approach – This paper explored developing and implementing process parameters for low-temperature wave soldering of Sn–Zn alloys (SN-9ZN-2.5BI-1.5 In). A two-factor, three-level design of the experiments experiment was designed to simulate various conditions parameters encountered in Sn–Zn soldering, developed the nitrogen protection device of waving soldering and proposed the optimal process parameters to realize mass production of low-temperature wave soldering on Sn–Zn alloys.

Findings – The Sn-9Zn-2.5 Bi-1.5In alloy can overcome the Zn oxidation problem, achieve low-temperature wave soldering and meet IPC standards, but requires the development of nitrogen protection devices and the optimization of a series of process parameters. The design experiment reveals that preheating temperature, soldering temperature and flux affect failure phenomena. Finally, combined with the process test results, an effective method to support mass production.

Research limitations/implications – In term of overcome Zn's oxidation characteristics, anti-oxidation wave welding device needs to be studied. Various process parameters need to be developed to achieve a welding process with lower temperature than that of lead solder(Sn–Pb) and lead-free SAC(Sn-0.3Ag-0.7Cu). The process window of Sn–Zn series alloy (Sn-9Zn-2.5 Bi-1.5In alloy) is narrow. A more stringent quality control chart is required to make mass production.

Practical implications – In this research, the soldering temperature of Sn-9Zn-2.5 Bi-1.5In is 5 °C and 25 °C lower than Sn–Pb and Sn-0.3Ag-0.7Cu (SAC0307). To the best of the authors' knowledge, this work was the first time to apply Sn–Zn solder alloy under actual production conditions on wave soldering, which was of great significance for the study of wave soldering of the same kind of solder alloy.

Social implications – Low-temperature wave soldering can supported green manufacturing widely, offering a new path to achieve carbon emissions for many factories and also combat to international climate change.

Originality/value – There are many research papers on Sn–Zn alloys, but methods of achieving low-temperature wave soldering to meet IPC standards are infrequent. Especially the process control method that can be mass-produced is more challenging. In addition, the metal storage is very high and the cost is relatively low, which is of great help to provide enterprise competitiveness and can also support the development of green manufacturing, which has a good role in promoting the broader development of the Sn–Zn series.

Keywords Sn–Zn solder, Low-temperature wave soldering, Lead-free solder, DOE

Paper type Research paper

1 Introduction

The European Union directive on e-waste management (restriction of the use of certain hazardous substances in

The current issue and full text archive of this journal is available on Emerald Insight at: **https://www.emerald.com/insight/0954-0911.htm**

Soldering & Surface Mount Technology
Emerald Publishing Limited [ISSN 0954-0911]
[DOI 10.1108/SSMT-11-2023-0064]

Received 4 November 2023
Revised 16 December 2023
30 December 2023
Accepted 30 December 2023

electrical and electronic equipment, RoHS) has drawn the attention of electronic producers worldwide to adopt the lead-free soldering system (Yin *et al.*, 2010). After the implementation of the RoHS legislation in 2006, electronic soldering materials have turned to lead-free solder (Cheng *et al.*, 2017), such as Sn–Ag–Cu (Bashir *et al.*, 2023; Long *et al.*, 2023; Yi *et al.*, 2023; Zhao *et al.*, 2002; Lin and Shih, 2008; Xu *et al.*, 2023), Sn–Cu (Lin *et al.*, 2018; Sarobol *et al.*, 2010; Skwarek *et al.*, 2021), Sn–Bi (Huang *et al.*, 2010; Miao and Duh, 2001; Wang *et al.*, 2013; Shaoan *et al.*, 2023) and Sn–Zn (Gong *et al.*, 2021; Gong *et al.*, 2022). Among the many solder alloys, the most widely used are SAC0307 (Yin *et al.*, 2010; Skwarek *et al.*, 2022) and, as a cheaper alternative, Sn–Cu (Snugovsky *et al.*, 2009) which the soldering temperature is 270°C and 280°C(hereafter, the temperatures that are not explicitly stated as board temperature are all setting temperatures). Sn–Zn solder alloy is also considered one of the most likely replacements for Sn–Pb solder alloys due to the similar melting temperature, greater mechanical strength and lower cost (Kotadia *et al.*, 2014). More significantly, lower soldering temperatures are more compatible with biodegradable printed circuit boards (PCBs), thus enhancing the environmental friendliness of the whole product (Honarbari *et al.*, 2023; Géczy *et al.*, 2022). However, the unsatisfactory wettability is still preventing the development of Sn–Zn solder alloy because of the oxidization (Islam *et al.*, 2005). Therefore, ZnO was successfully used to manufacture the SAC0307 solder alloys (Skwarek *et al.*, 2021; Skwarek *et al.*, 2022). Until recent studies, it was still impossible to solve the wettability problem (Chen *et al.*, 2018).

Ren (Ren *et al.*, 2022) has demonstrated that adding nitrogen protection to wave soldering equipment effectively avoids oxidation in the laboratory. Chen (Chen *et al.*, 2006; Wu *et al.*, 2003) shows that adding trace elements to Sn–Zn alloy can improve the wettability and oxidation resistance, and ensure solder quality by controlling intermetallic compound growth. Therefore, it allows the realization of Sn–Zn soldering alloy wave soldering under industrial production conditions. The alloy of Sn-9Zn-2.5 Bi-1.5In lead-free solder was designed to apply with the soldering temperature (Gong *et al.*, 2023) of 215°C which is lower than 260°C–265°C of Sn–Ag–Cu alloy and 270°C–275°C of Sn–Cu (Lin *et al.*, 2018) alloy. Besides, the solder material, which affects the application of the PCB board, the soldering process parameters also play a crucial role (Seidel *et al.*, 2021). Therefore, verifying whether wave soldering of Sn–Zn alloys can meet the IPC standards A-610H-CN 2017–10 (Task Group (7—31 b), Task Group Asia (7 — 31bCN) and Task Group Nordic (7 — 31bND) of the Product Assurance Committees (7—30 and 7 — 30CN) of IPC) is of great interest.

In this study, components of a computer motherboard were soldered by using Sn-9Zn-2.5 Bi-1.5In alloy as a lead-free solder alloy in wave soldering equipment containing nitrogen gas protection. X-RAY and metallurgical microscopy analyzed the components and their cross-sections, and the optimal process parameters with the least defect rate were found using the DOE (design of the experiments) method, proving that Sn–Zn solder alloys can be manufactured for wave soldering.

2 Experimental method

2.1 Experimental materials

The solder alloy used for the experimental wave soldering was Sn-9Zn-2.5 Bi-1.5In, purchased from Beijing Lianjin New Material Technology Co., Beijing, China. All the alloys were processed into bar shape to facilitate the timely replenishment of the missing solder in the wave soldering furnace. The melting conditions were: using a resistance furnace under argon protection for melting, holding the metal at 300°C for 1 h after complete melting and then cooling to 280°C for pouring to form a bar. The elemental content, melting point and density of the alloy are shown in Table 1.

The motherboard used for the experiment is a PCB board, which had already been heavily used as a computer motherboard in the existing Sn–Ag–Cu wave soldering production. The motherboard was red copper, and the organic solderability preservatives (OSP) finish processed the surface. Components on the substrate included USB interfaces, memory banks, pin headers, diodes, resistors, capacitors, etc. All components were hand-assembled during the experiment in full accordance with the existing SAC0307 wave soldering production process.

To get the exact difference between the set temperature and the actual soldering temperature of each motherboard section, a temperature data logger (purchased from OMEGA ENGINEERING, Inc., Norwalk, America) and a specialized temperature measurement board were used to measure the induced temperature in various main parts. The red epoxy glue attached the type K thermocouples to the temperature measurement board. The actual board temperature of eight points shown in Table 2 was measured to search for more details on various components' temperature requirements. A schematic diagram of connecting thermocouple is provided in below Figure 1.

Three types of flux composition, HF18, HF27 and HF28, were selected in this study, which were halogen-free and no-clean fluxes for lead-free solder. All three fluxes were cooperative development from COSTAR ELECTRONIC

Table 1 Sn-9Zn-2.5 Bi-1.5 in alloy property

Melting point (°C)	Melting range (°C)	Density (g/cm^3)	Electrical conductivity (S·m^{-1})	Shear strength (MPa)
194	4	7.28	7.6	65

Source: Created by author

Table 2 The positions and the types of temperature measurement

Position	Type
1	Liquid alloy
2	Connector F_AUDIO
3	USB
4	SYS_ARGB
5	Capacitor PC920
6	Capacitor PC624
7	SATA Conn.
8	SIDE1 Conn.

Source: Created by author

Figure 1 Schematic diagram of connecting thermocouple

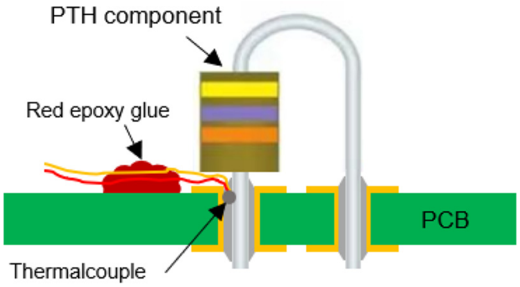

Source: Created by author

MATERIAL. CO. LTD had a solid content of 3.7% and a rosin content of 1.2%, but the acid value of HF18 was 23.5, that of HF27 was 27.7 and that of HF28 was 29.

2.2 Experimental equipment

SMART-450MO-N wave soldering equipment produced by SHENZHEN JT AUTOMATION EQUIPMENT CO. LTD. was used in the experiment, which installed a self-developed nitrogen protection system. The solder pot had a capacity of 450 kg, and the preheating area was divided into four sections, each with a length of 780 mm. To make the whole soldering process conducted in a relatively low oxygen environment, a nitrogen sampling port overlays the entire soldering area. Three nitrogen gas pipes in the front, the middle and the back of Wave One and Wave Two were installed to let the gas continuously fill the nitrogen sampling port with high-purity nitrogen to maintain the low oxygen content in the sampling port.

In addition, each sample was tested by XD7500VR X-RAY (purchased by Dage Test Systems (Suzhou) Co. Ltd., Suzhou, China), and the cold inlaid sample was ground by YMPZ-2 automatic grinding machine (purchased from Shanghai Metallurgical Equipment Company Ltd., Shanghai, China). The ground sample was observed by an Olympus BX53MTRF-S metallographic microscope (purchased from Nikon Imaging (CHINA) Sales Co. China).

2.3 Experimental methodology

It was necessary to set the preheating and furnace temperature during the experiment. Because of the many process parameters of wave soldering and the variety and complexity of the causes of defects, this research adopted the DOE method, which first needs to determine the factors and levels through process experiments, as shown in Table 3. Each experiment was conducted using one motherboard with 507 active solder joints. Eight couples of the thermocouples were connected to the corresponding area of the temperature measurement board. The temperature measurement board with thermocouples and samples was put on the transmission chain grab of the wave soldering equipment. The transmission chain grab would drive the temperature measurement board and samples through the four preheating zones and Wave Two. The soldered samples were first sent to X-RAY for inspection and then were split into small pieces by a precision cutting machine for cold mounting. After grinding and polishing, the metallurgical microscope would observe the cross-section.

According to the process experiment results, track speed and preheating temperature were selected for DOE experiments. Each experiment used five motherboards to eliminate the error and produced 2,535 practical solder joints. The experimental program is shown in Table 4.

As experience and the production process requirement, scoring on soldering defects is a way to verify the quality of the wave soldering. Scoring is to evaluate each process group to search for the most suitable ones. The more it scores, the more detects occur. According to internal quality assurances such as the level of repairing and even second-time soldering, it is recommended to score 0.2, 0.3, 0.3, 0.5 and 0.7, respectively, on the defects of solder bridging, floating pieces, insufficient filling 50%–75%, 30%–50% and less than 30%.

2.4 Soldering quality criteria

According to industry process requirements and IPC standards A-610H-CN 2017–10, wave solder filling requirements vary by type and function. This standard considers less than 75% of solder filling a defect. Solder filling between 50% and 75% is tolerated in components that do not require high reliability. The solder-filling level schematic is shown in Figure 2(a). The typical defects of wave soldering, which appeared at the early start of the projects, are shown in Figure 2(b)–(c). Because bridging may lead to component short-circuiting, floating pieces of the probability of not being able to assemble and serious insufficient solder filling can lead to leakage of soldering, leading to component breakage, the three defects will

Table 3 Process experiment programs

Factors	Levels	Other conditions
Soldering temperature	230°C	Flux: HF18
	240°C	Preheating temperature: 160°C
	250°C	Track speed: 1100 mm/min
Preheating temperature	150°C	soldering temperatures: 250°C
	160°C	Flux: HF18
	170°C	Track speed: 1100 mm/min
	180°C	
The style of flux	HF18	soldering temperatures: 250°C
	HF27	Preheating temperature: 160°C
	HF28	Track speed: 1100 mm/min

Source: Created by author

Table 4 DOE experiments program

	Factors	
Group no.	Preheating temperature(°C)	Track speed(mm/min)
1	155	900
2	155	1050
3	155	1200
4	163	900
5	163	1050
6	163	1200
7	170	900
8	170	1050
9	170	1200

Source: Created by author

Figure 2 Solder filling level schematic (a) and X-Ray (b) and cross-section (c) of solder joint bubble

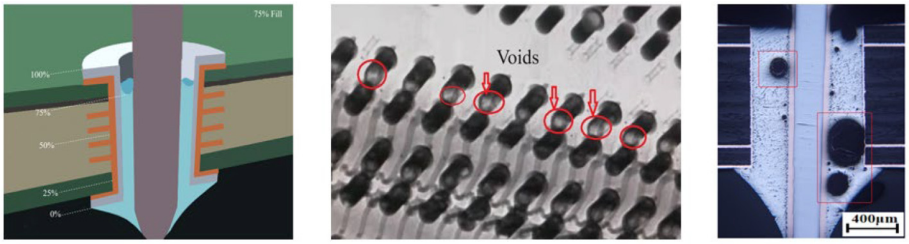

(a) **(b)** **(c)**

Source: Created by author

directly affect the function and reliability of the motherboard, compared with other defects extra significant. Therefore, these three defects are used to study in this paper, in which the bridging, floating pieces and some of the very poor insufficient solder filling are obvious and can be directly observed by the naked eye. Still, all of them need to be examined by X-RAY and slicing.

3 Results and discussion

3.1 Soldering temperature

Due to the ground layer of the PCB board having a large copper layer, which can conduct heat fast, the temperature of soldering feet is transferred to the ground layer quickly. Therefore, the general use of large-size capacitor pins for the soldering temperature test object. In this experiment, Position 5 was the position of the large-size capacitor, which was selected to study the actual temperature measured and the soldering joint results. The actual temperature shown in Table 5 also demonstrates that the peak temperature of Position 5 is the lowest of the eight points. The X-rays are shown in Figure 3, and the cross-sections are shown in Figure 4. The number of defects of bridging, floating pieces and insufficient solder filling are listed in Table 6.

A cylindrical shadow pointed by red arrows can be seen in Figure 4, which outlines the PCB's through-hole. The shadow surrounded by a red circle is the solder alloy. The larger the shadow, the better the soldering. Figures 3 and 4 show that the solder alloy in the through-hole becomes more abundant as the temperature increases. The defects appeared at board temperatures below 230°C because the temperature at Position 5 does not reach the soldering temperature of the solder alloy. As the temperature increases, the amount of tin on each pin rises. This is a direct indication that the increase in temperature benefits the Sn–Zn solder in forming a metallurgical bond with the metal on the component's surface. In addition, as the temperature increases, the number of floating pieces decreases gradually and the value of insufficient solder filling decreases significantly at all levels, indicating that the increase in soldering temperature is favorable to reducing the generation of floating pieces and insufficient solder filling. This is because, during the soldering process, the component will inevitably flow due to the disturbance of the liquid solder advection wave. After leaving the advection wave, the component will naturally fall back to its initial position under the influence of gravity. However, if the temperature of the solder alloy has fallen below the melting point during the fallback process, the solidified solder alloy will hold the component in one of the falling positions, producing a floating piece. When the setting temperature exceeds 250°C, the board temperature at the large capacitor can reach 230°C. This ensures that the solder alloy will not fall below 195°C before the component returns to the initial position. Therefore, it will significantly reduce the probability of floating pieces being generated. Furthermore, the number of bridging does not decrease, suggesting that the lack of metallurgical bonding between the component and the solder does not cause bridging. Therefore, it is not related to the soldering temperature. The result shows that a higher soldering temperature provides better suitable soldering results with fewer defects. The experiment could not continue to raise the soldering temperature because the defects had already met the IPC standards, and the oxidation of the solder alloy increased dramatically during the soldering process. In the process of raising the temperature, a film appeared on the surface of the tin wave inside the nitrogen sampling port, and this tin film would hang on the pins during soldering, resulting in insufficient solder filling. A large dross would also be produced rapidly in the tin furnace outside the nitrogen hood, creating a considerable loss of raw materials. Therefore, 250°C of setting soldering temperature was chosen for this study to conduct the rest of the experiments. Meanwhile, the actual board temperature is only 231.8°C which is 5°C lower than the Sn–Pb solder alloy, and more than 20°C lower than other alloys such as Sn–Ag–Cu and Sn–Cu (Forstén *et al.*, 2000).

Table 5 The peak temperature and contact time of the temperature measurement points

Position	Type	Peak temperature(°C)	Contact time(s)
1	Liquid alloy	244.4	5
2	Connector F_AUDIO	240.2	5
3	USB	237.7	5
4	SYS_ARGB	238.9	5
5	Capacitor PC920	231.8	6
6	Capacitor PC624	241.0	5
7	SATA Conn.	240.5	6
8	SIDE1 Conn.	242.6	4

Source: Created by author

Figure 3 Cross-sections of different (230°C (a)0.240°C(b), and 250°C(c)) soldering temperature

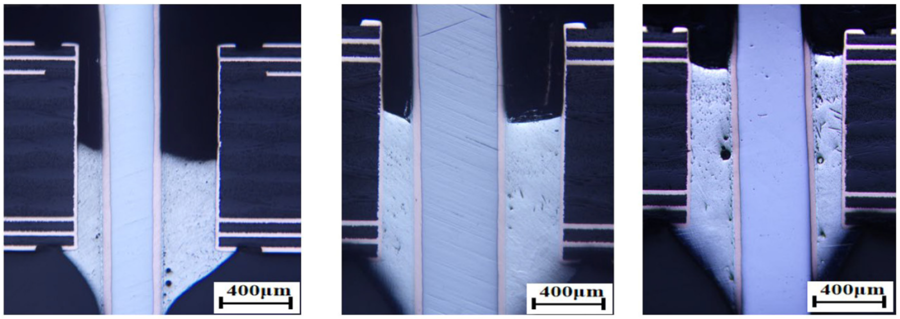

(a) **(b)** **(c)**

Source: Created by author

Figure 4 X-ray of different (230°C (a)0.240°C(b), and 250°C(c)) soldering temperature

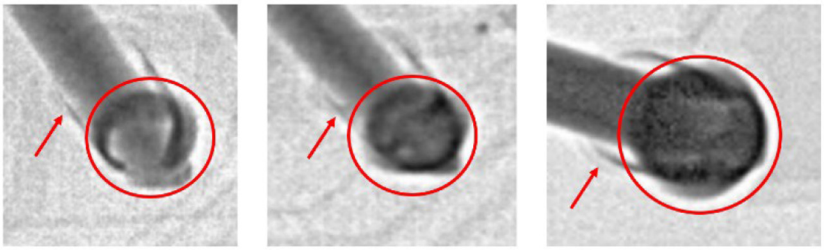

(a) **(b)** **(c)**

Source: Created by author

Table 6 Total defects of soldering temperature process experiment

Soldering temperature (°C)	Bridging	Floating piece	Insufficient solder filling 50%–75%	30%–50%	<30%
230	12	12	15	8	6
240	10	9	9	5	3
250	12	4	5	1	0

Source: Created by author

3.2 Preheating temperature

The furnace temperature profiles are shown in Figure 5, and the sample pictures are shown in Figure 6. The number of defects of the preheating temperature process experiment is listed in Table 7.

Figure 5 proves that the actual peak board temperature is only 99.5°C. Therefore, 150°C of preheating temperature results from bridging and solder ball defects more than others because it is too low to remove the oxide film on the surface of the solder alloy. Therefore, when the flux is heated, rapidly vaporizes and expands to break through the oxide film, tiny tin droplets will fly out along with the flux vapor that fall on the PCB board to form solder balls. The flux activity increases as the temperature rises, making it more favorable to react with the solder during the soldering process. This phenomenon is evidenced by the results of soldering at 160°C and 170°C, but too high a temperature results in the acid being broken down, resulting in deactivation of the flux, which provokes defects of insufficient solder filling such as 180°C (Piotrowska *et al.*, 2017). In comparison, preheating temperatures of 160°C and 170°C provide fairly good solder filling without defects. The PCB boards are clean without solder balls, demonstrating the feasibility of Sn–Zn wave soldering.

Figure 5 The furnace temperature profile of the preheating temperature process experiment

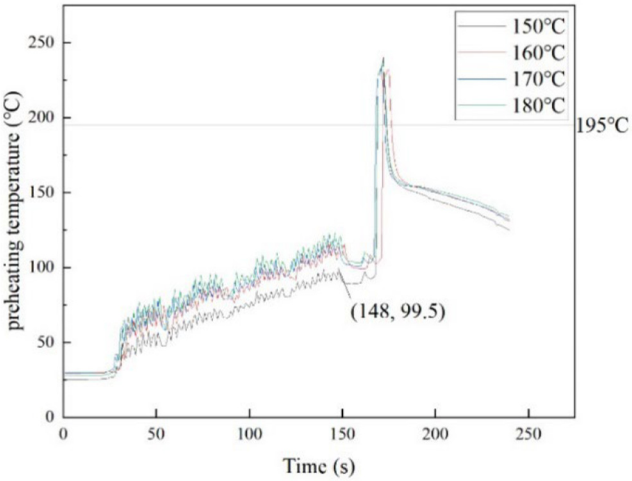

Source: Created by author

Figure 6 The pictures of the sample of different (150°C (a), 160°C(b), 170°C(c) and 180°C(d)) preheating temperature

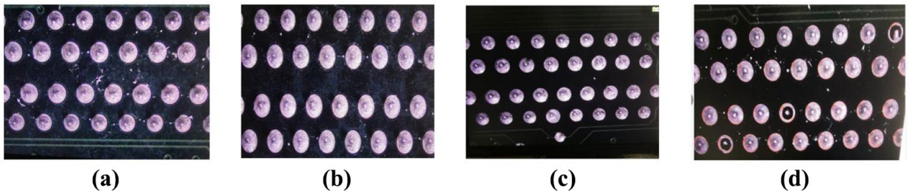
(a) (b) (c) (d)

Source: Created by author

Table 7 Total defects of preheating temperature process experiment

Preheating temperature(°C)	Bridging	Floating piece	Insufficient solder filling 50%–75%	30%–50%	<30%
150	15	6	8	6	0
160	8	5	4	4	0
170	5	5	4	2	0
180	18	6	12	8	0

Source: Created by author

Figure 7 X-ray of different (HF18 (a), HF27 (b), and HF28 (c)) flux

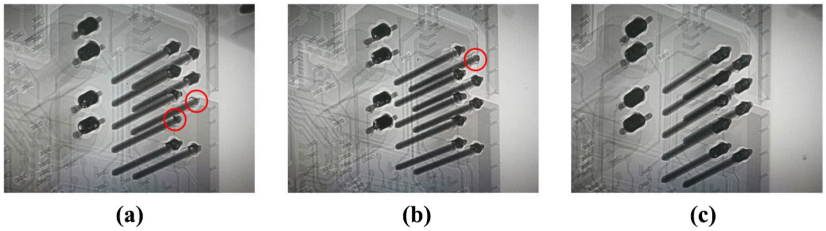
(a) (b) (c)

Source: Created by author

Table 8 Total defects of flux optimization process experiment

Flux	Bridging	Floating piece	Insufficient solder filling 50%–75%	30%–50%	<30%
HF18	13	4	12	5	3
HF27	9	6	8	4	0
HF28	4	4	4	1	0

Source: Created by author

3.3 Flux optimization

The X-rays are shown in Figure 7. The number of defects in the track speed process experiment is listed in Table 8.

The role of flux activators in flux formulation is to remove oxides from metal surface and, hence, allow the formation of the metallurgical bond between metal substrate and solder alloy. Therefore, an essential property of flux activators is the acid value. The higher the acid value, the better the activation effect and the more helpful it is for soldering. However, too high an acid value can lead to poor flux preservation, and the residue of no-clean flux can also corrode the solder alloy at the solder joint, resulting in poor reliability, so the acid value should not be too high either. Sn–Zn solder alloy wetting on Ni has always been an important issue in research. The current research can rarely be seen between Sn–Zn solder alloy and Ni elements of the combination. The soldering effect on nickel-plated components in production is even more rare. In the experiment, the components at position 2, F_AUDIO, are nickel-plated and then slightly gold-plated. During the production process, the gold-plated layer tends to wear out due to the transfer, resulting in the nickel-plated layer being exposed. Thus, it can be regarded as a nickel-plated component.

During early studies, F_AUDIO had poor wetting, but as the fluxes improved on the acid value, the HF18 fluxes could meet the production requirements' bottom line. However, there were still 13 bridging and 8 substandard insufficient solder fillings, as shown in Table 8. Figure 7(a) also showed that there were still some insufficient solder fillings. As the acid value rises, HF27 significantly improves over HF18 in bridging and insufficient solder filling, and HF28 has the best results, with only 4 bridging and 1 insufficient solder filling, and not less than 30% of insufficient solder filling.

Table 9 The scores of the DOE

Group no.	Parameters	Total pins for bridging	Total pins for floating pieces	Total pins for insufficient solder filling	Overall defects score
1	155–900	86	23	5	26.8
2	155–1050	48	29	13	22.8
3	155–1200	33	22	18	20.4
4	160–900	80	6	6	20
5	160–1050	9	14	21	13.5
6	160–1200	9	6	30	15.2
7	170–900	25	5	17	13.8
8	170–1050	10	4	16	8.8
9	170–1200	3	7	22	11.5

Source: Created by author

Figure 8 X-rays and cross-sections of different components (a-Connector JPE1, b-Capacitor PC624, c-Capacitor PC920, d- Connector JU3R1,)

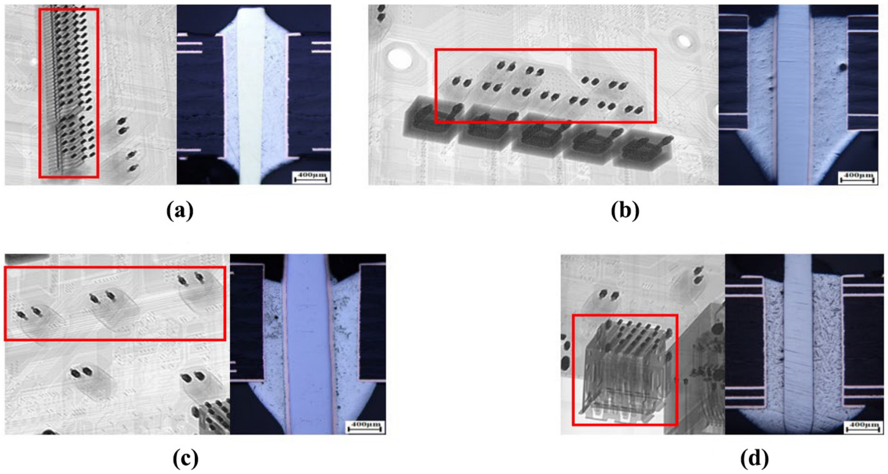

(a) (b)

(c) (d)

Source: Created by author

3.4 Design of the experiments discussion

There are very many factors affecting the effect of wave soldering. Therefore, there is a need to improve the process using the DOE method to obtain combinations of parameters consistent with mathematical statistics through a relatively small number of experiments. In the previous study, the soldering temperature and flux have been determined; only the track speed and preheating temperature required further discussion. To obtain the best process parameters, a list of factors and levels was composed in Table 4 and the scores of the DOE are shown in Table 9.

The 9-group experiment results in Table 9 prove that the preheating temperature is the more important of the two factors. Track speed is also essential but is a secondary factor with a wide permissible range from 900 mm/min to 1200 mm/min.

Therefore, after comprehensively considering the reliability and the difficulty of repair, the preheating temperature of 170°C, track speed of 1050 mm/min, the soldering temperature of 250°C and HF28 flux are considered to be the most suitable process parameters for Sn–Zn wave soldering. From the X-RAY results in Figure 8, it can be seen that the soldering results of all the components are very satisfactory, with a sufficient amount of tin and the slicing results show that the solder alloy in the through-hole is uniformly organized, without bubbles and is tightly bonded to the components.

4 Conclusion

It is the first time that a low-temperature lead-free solder alloy, Sn-9Zn-2.5 Bi-1.5In, and wave soldering equipment with nitrogen protection were prepared for new design process parameters. Having solved the problem of oxidation of Zn, Sn-9Zn-2.5 Bi-1.5In was proven to be a low-temperature alloy with advantages such as low density, low melting point and good wettability, which meet the IPC standards. The board temperature is 15°C lower than Sn–Ag–Cu and 25°C lower than Sn–Cu, reducing the production period cost and electric consumption. Meanwhile, the process parameters are also significant to those planning to use Sn-9Zn as wave soldering alloy. The following conclusions can be made based on the above analysis:

- Sn–Zn solder alloy can be industrially produced on existing wave soldering equipment with nitrogen protection, with a defect rate that meets IPC standards A-610H-CN 2017-10. It has a lower soldering temperature than Sn–Pb, Sn–Ag–Cu and Sn–Cu solder alloys.

- Higher soldering temperatures, preheating temperatures and flux acid values can reduce the probability of defects within a suitable interval. In DOE, preheating temperature was a more critical factor than track speed and played a decisive role in soldering results.
- The preheating temperature of 170°C, track speed of 1050 mm/min, the soldering temperature of 250°C and HF28 flux are considered the most suitable process parameters for Sn–Zn wave soldering. The defect rate for defects is 0.30% for bridging, 0.16% for floating pieces and 0.63% for insufficient solder filling.

References

Bashir, M.N., Khan, A.F., Bashir, S., Bashir, M.B.A., Jamshaid, M., Javed, I. and Ali, I. (2023), "Effect of Zn nanoparticle doped flux on electromigration damages in SAC305 solder joint", *Journal of Materials Science-Materials in Electronics*, Vol. 34.

Cheng, S., Huang, C.-M. and Pecht, M. (2017), "A review of lead-free solders for electronics applications", *Microelectronics Reliability*, Vol. 75, pp. 77-95.

Chen, G., Li, X. and Mai, J. (2006), "Effect of thermal cycling on the growth of intermetallic compounds at the Sn-Zn-Bi-in-P lead-free solder/Cu interface", *Journal of Electronic Materials*, Vol. 35 No. 10, pp. 1873-1878.

Chen, Y., Wang, Z., Ma, J. and Zhang, G. (2018), "Application of Sn-Zn lead-free solder on wave soldering", *Electronic Components & Materials*, Vol. 37, pp. 8-13.

FORSTéN, A., Steen, H., Wilding, I. and Friedrich, J. (2000), "Development and validation of lead-free wave soldering process", *Soldering & Surface Mount Technology*, Vol. 12 No. 3, pp. 29-34.

Géczy, A., farkas, C., Kovács, R., Froš, D., Veselý, P. and Bonyár, A. (2022), "Biodegradable and nanocomposite materials as printed circuit substrates: a mini-review", *IEEE Open Journal of Nanotechnology*, Vol. 3, pp. 182-190.

Gong, S., Chen, G., Qu, S., Duk, V., Shi, Q. and Zhang, G. (2021), "Shear strength and fracture analysis of Sn-9Zn-2.5Bi-1.5In and Sn-3.0Ag-0.5Cu pastes with Cu-substrate joints under different reflow times", *Microelectronics Reliability*, Vol. 127, p. 114378.

Gong, S., Zhang, G. and Ren, A. (2022), "Contrastive study on shear strength and fracture mechanism of Sn-9Zn-2.5Bi-1.5In and Sn-3.0Ag-0.5Cu solder joints with aging treatment", *2022 23rd International Conference on Electronic Packaging Technology (ICEPT)*, p. 5.

Gong S. Chen G. Qu S. Xu X. Duk V. Shi Q. and Zhang G. (2023), "Microstructure evolution and mechanical properties of Sn-9Zn-2.5Bi-1.5In solder joints with aging treatment under various conditions", *Materials Characterization*, Vol. 205, p. 113319.

Honarbari, A., Cataldi, P., Zych, A., Merino, D., Paknezhad, N., Ceseracciu, L., Perotto, G., Crepaldi, M. and Athanassiou, A. (2023), "A green conformable thermoformed printed circuit board sourced from renewable materials", *ACS Applied Electronic Materials*, Vol. 5 No. 9, pp. 5050-5060.

Huang, Y.-C., Gierlotka, W. and Chen, S.-W. (2010), "Sn-Bi-Fe thermodynamic modeling and Sn-Bi/Fe interfacial reactions", *Intermetallics*, Vol. 18 No. 5, pp. 984-991.

Islam, M.N., Chan, Y.C., Rizvi, M.J. and Jillek, W. (2005), "Investigations of interfacial reactions of Sn–Zn based and Sn–Ag–Cu lead-free solder alloys as replacement for Sn–Pb solder", *Journal of Alloys and Compounds*, Vol. 400 Nos 1/2, pp. 136-144.

Kotadia, H.R., Howes, P.D. and Mannan, S.H. (2014), "A review: on the development of low melting temperature Pb-free solders", *Microelectronics Reliability*, Vol. 54 Nos 6/7, pp. 1253-1273.

Lin, K.-L. and Shih, P.-C. (2008), "IMC formation on BGA package with Sn-Ag-Cu and Sn-Ag-Cu-Ni-Ge solder balls", *Journal of Alloys and Compounds*, Vol. 452 No. 2, pp. 291-297.

Lin, Q., Li, F. and Wang, J. (2018), "Wetting of Sn/Cu and Sn/Cu-Sn IMCs at 623-723K", *Journal of Alloys and Compounds*, Vol. 767, pp. 877-882.

Long, X., Guo, Y., Su, Y., Siow, K.S. and Chen, C. (2023), "Unveiling the damage evolution of SAC305 during fatigue by entropy generation", *International Journal of Mechanical Sciences*, Vol. 244, p. 108087.

Miao, H.W. and Duh, J.G. (2001), "Microstructure evolution in Sn-Bi and Sn-Bi-Cu solder joints under thermal aging", *Materials Chemistry and Physics*, Vol. 71 No. 3, pp. 255-271.

Piotrowska, K., Jellesen, M.S. and Ambat, R. (2017), "Thermal decomposition of solder flux activators under simulated wave soldering conditions", *Soldering & Surface Mount Technology*, Vol. 29 No. 3, pp. 133-143.

Ren, A., Dong, X., Shi, Q., Zhang, G. and Zhu, Z. (2022), "Effect of O_2 content on soldering quality in Sn-9Zn-2.5Bi-1.5In low-temperature wave soldering", *Transactions of the China Welding Institution*, Vol. 43 No. 99, pp. 68-73.

Sarobol, P., Pedigo, A.E., Su, P., Blendell, J.E. and Handwerker, C.A. (2010), "Defect morphology and texture in Sn, Sn-Cu, and Sn-Cu-Pb electroplated films", *IEEE Transactions on Electronics Packaging Manufacturing*, Vol. 33 No. 3, pp. 159-164.

Seidel, R., Sippel, M., Franke, J. and Soc, I.C. (2021), An Analytical Approach to Thermal Design for Manufacturing in mini wave Soldering, *IEEE 71st Electronic Components and Technology Conference (ECTC)*, 2021 Jun 01-Jul 04 2021 Electr Network, pp. 1427-1434.

Shaoan, W., Xiangyu, C., Keyu, L., Hongzhi, Z., Rongqing, L., Peng, H., Kyung-Wook, P. and Shuye, Z. (2023), "The design of low-temperature solder alloys and the comparison of mechanical performance of solder joints on ENIG and ENEPIG interface", *Journal of Materials Research and Technology*.

Skwarek, A., Krammer, O., Hurtony, T., Ptak, P., GóRECKI, K., Wronski, S., Straubinger, D., Witek, K. and ILLéS, B. (2021), "Application of ZnO nanoparticles in Sn99Ag0.3Cu0.7-based composite solder alloys", *Nanomaterials*, Vol. 11 No. 6, p. 11.

Skwarek, A., Ptak, P.P., GóRECKI, K., Witek, K. and ILLéS, B. (2022), "The influence of SACX0307-ZnO nanocomposite solder alloys on the optical and thermal properties of power LEDs", *Soldering & Surface Mount Technology*, Vol. 34 No. 4, pp. 222-229.

Snugovsky, P., Bagheri, Z. and Hamilton, C. (2009), “Microstructure and reliability comparison of different Pb-Free alloys used for wave soldering and rework”, *Journal of Electronic Materials*, Vol. 38 No. 12, pp. 2628-2646.

Wang, X., Chen, Y., Chen, Q., Luo, D., Liu, N. and Wang, F. (2013), “Analysis of Sn-Bi solder joint blacking”, *Electronic Components & Materials*, Vol. 32, pp. 37-40.

Wu, C.M.L., Law, C.M.T., Yu, D.Q. and Wang, L. (2003), “The wettability and microstructure of Sn-Zn-RE alloys”, *Journal of Electronic Materials*, Vol. 32 No. 2, pp. 63-69.

Xu, S.W., Jing, X.Y., Zhu, P.Y., Jin, H.R., Paik, K.W., He, P. and Zhang, S.Y. (2023), “Equilibrium phase diagram design and structural optimization of SAC/Sn-Pb composite structure solder joint for preferable stress distribution”, *Materials Characterization*, Vol. 206, p. 113389.

Yi, P., Chen, D., Li, M., Yang, Z., Fang, Z., Mo, J., Xiao, K. and Dong, C. (2023), “Effect of Nd addition on the corrosion behavior of SAC305 solder alloy”, *Corrosion Science*, Vol. 220, p. 111264.

Yin, F.F., Zhang, X.H., Wang, H.L., Yu, S.R. and Selected, P. R.P.F.T.I.O. (2010), “Optimization of process parameters in lead-free wave soldering based on orthogonal experiment and analytic hierarchy process”, *Applied Mechanics and Materials*, Vol. 26-28, pp. 641-647.

Zhao, J., Mutoh, Y., Miyashita, Y. and Mannan, S.L. (2002), “Fatigue crack-growth behavior of Sn-Ag-Cu and Sn-Ag-Cu-Bi lead-free solders”, *Journal of Electronic Materials*, Vol. 31 No. 8, pp. 879-886.

Corresponding author

Songtao Qu can be contacted at: Songtao.Qu@lcfuturecenter.com